Mendeleev Commun., 2027, **37**, JUST ACCEPTED

Received 30.09.26 26/8216

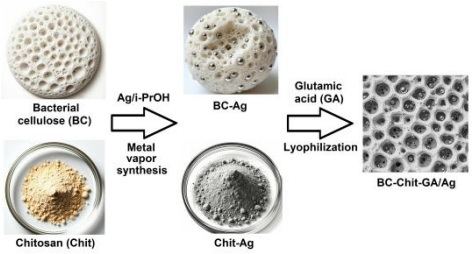
Synthesis and structure of silver-containing bacterial cellulose composites with chitosan

Ivan E. Butenko, Polina R. Voloshina, Alexander V. Naumkin, Alexandre S. Golub and Alexander Yu. Vasil'kov*

A. N. Nesmeyanov Institute of Organoelement Compounds, Russian Academy of Sciences, 119334 Moscow, Russian Federation. E-mail: alexandervasilkov@yandex.ru

DOI: 10.71267/mencom.8216

Porous silver-containing materials promising for medical applications have been obtained using bacterial cellulose, chitosan, and glutamic acid. The composites were prepared using a combination of metal-vapor synthesis, gelation, and freeze-drying. The silver in the composite exists in both Ag^0 and Ag^+ states, and the silver crystallite size is 21.5 nm.



Keywords: bacterial cellulose, chitosan, glutamic acid, silver nanoparticles, metal–vapor synthesis, XRD, XPS.

Development of effective medical materials based on biocompatible natural polymers and biologically active metal nanoparticles that provide prolonged antimicrobial action is an extremely important and rapidly developing area of research. Its relevance is caused by the overuse of antibiotics and the increasing resistance in microorganisms which reduces the effectiveness of wound healing using previously developed medications.[1,2] Nanoparticles of biologically active metals and their oxides may be an alternative to antibiotics as they do not induce bacterial resistance. For successful wound healing the covering material must not only have antimicrobial activity but also stimulate tissue regeneration.[3,4] There is an active growth of publications on the preparation of hybrid materials dedicated to the integration of biologically active metal nanoparticles into bacterial cellulose (BC)[5,6], chitosan (Chit)[7,8] and hybrid material based on them (BC-Chit).[9,10]

These polysaccharides are biocompatible, non-toxic and biodegradable which is why they are widely used in medicine.[11, 12]

Bacterial cellulose synthesized by microorganisms is characterized by high purity, a nanofibrillar structure, mechanical strength, and biocompatibility. Thanks to an extensive network of hydrogen bonds and a large specific surface area, bacterial cellulose interacts effectively with various fillers, making it a promising matrix for the creation of composite materials.

Chitosan's hemostatic properties facilitate the use of fibrous materials derived from it as hemostatic dressings. Featuring an open-pore structure, these materials swell significantly in biological fluids—transforming into a gel—and conform tightly to the wound.

Despite its important properties for medical materials, cellulose is susceptible to microbial contamination, and chitosan becomes brittle after excessive water absorption and is not suitable for wound-healing dressings.[13, 14] Synthesis of a composite based on chitosan and cellulose can compensate for their shortcomings and lead to the preparation of a material that combines the physicochemical and antimicrobial properties of chitosan and the mechanical properties of cellulose.[10,15]

The most common method for producing BC-Chit composites is impregnation of BC with a solution of chitosan in acetic acid.[10,16] However the final product contains cytotoxic residues. The use of glutamic acid (GA) as a solvent and cross-linking agent of chitosan has several advantages comparing to other existing methods due to its biocompatibility, biodegradability and the ability to stimulate collagen production during wound healing.[17]

It has been established that silver nanoparticles (Ag NPs) and their composites with BC and Chit exhibit biological activity with a broad spectrum of action against various strains of microorganisms resistant to antibiotics.[8,9,10]

This study presents the production of porous Ag-containing hybrid materials based on the BC-Chit composite using several technological processes: metal-vapor synthesis (MVS), gelation, and lyophilization (Figure S1).

The bacterial cellulose used was obtained by dynamic cultivation. It is a gel-like system consisting of irregularly shaped granules. Compared to the BC film, it has a larger surface area, a three-dimensional network structure, and a high release rate of loaded biologically active substances.[18]

Ag NPs were prepared with MVS, which is actively used to produce hybrid metal-containing composites for biomedical purposes.[8,19-22] The key advantage of this method is the absence of byproducts in the metal nanoparticles which is very important for ensuring the purity of medical materials.

In the first step BC and Chit were modified with Ag NPs-isopropanol organosol synthesized by the MVS, yielding BC@Ag and Chit@Ag composites.

In the second step a gel-like system was formed from the metal-containing composites in a glutamic acid solution, from

© Mendeleev Communications.

which a porous hybrid material BC-Chit-GA@Ag was obtained by lyophilization. The morphology of BC, BC-Chit-GA and BC-Chit-GA@Ag was investigated by SEM (Figure 1 a-c). It was established that the BC obtained by dynamic cultivation (Figure 1a) has a network microfibril structure characteristic of this polymer.[23,24] Individual fibrils with a diameter of 15–30 nm tend to form large intertwined domains with a diameter of 60 to 120 nm. Comparative analysis of BC-Chit-GA and BC-Chit-GA@Ag composites showed that the structures of the materials after lyophilization are similar and the injection of Ag NPs has virtually no effect (Figure 1b and c). Apparently, during the synthesis process, the fibrils and cavities of the BC, which forms the framework of the material, are filled with the Chit-GA@Ag composite to form a three-dimensional porous structure containing strands, plates, and cavities.

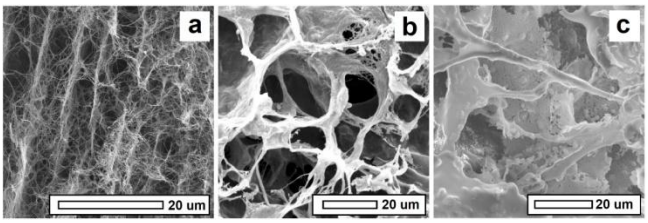


Figure 1 SEM images of the morphology of BC (a), BC-Chit-GA (b) and BC-Chit-GA@Ag (c)

SEM/EDX data analysis allowed us to determine the composition and presence of Ag in the BC-Chit-GA@Ag sample and showed a uniform distribution of the metal throughout the volume of the material (Figure S2, S3).

The thermal stability of BC-Chit-GA and BC-Chit-GA@Ag composites was investigated using thermogravimetric analysis (Fig. S4). It was found that the incorporation of Ag NPs does not reduce the thermal stability of the Ag-containing composite, which is important for the sterilization of medical materials.

The XRD was used to study the samples of BC, Chit, BC-Chit-GA and BC-Chit-GA@Ag, the diffraction patterns of which are presented in Figure 2. The diffraction profile of BC (Figure 2a) is well described by the allomorph Iα of cellulose with the most intense diffraction peaks located at 14.4° (010), 16.7° (001) and 22.5° (011), which are consistent with the literature data.[24,25] The more amorphous Chit (Figure 2b) gives a broad asymmetric reflection in the region under consideration with a maximum at ~20.0° 2θ and an unresolved satellite at ~22.3° 2θ.[26] In contrast to BC and Chit, GA produces a set of numerous narrow diffraction peaks (Figure 2c). All of them correspond to the orthorhombic lattice of the stable β-form of L-glutamic acid (CSD refcode LGLUAC01, sp. gr. P212121, a=5.154 Å, b=6.942 Å, c=17.274 Å, and α=β=γ=90°). The diffraction pattern of the BC-Chit-GA composite (Figure 2d) shows a dominant contribution of BC, supplemented by low-intensity peaks of GA while the contribution of Chit is almost imperceptible. In the case of the BC-Chit-GA@Ag composite (Figure 2e) the diffraction pattern is dominated by the face-centered cubic phase of metallic Ag (sp. gr. Fm-3m, a= 4.0862 Å, COD number 9008459) due to its strong peaks appearing at 38.11° (111), 44.43° (002), 64.44° (022), 77.40° (311), and 81.54° (222). The contribution of BC and GA in the BC-Chit-GA@Ag hybrid material can be determined from their weak reflections in the small-angle region. To determine the crystallite size (D) of Ag nanoparticles in this composite, Rietveld refinement of the diffraction profile in the 2θ > 35° region containing the Ag reflections was performed. The crystallite size of Ag nanoparticles, averaged over different crystallographic directions, was calculated using the calculated diffraction pattern and the Scherrer dependence: D = 0.89 λ/(b cos θ), where λ is the X-ray wavelength, b and θ are the full width at half maximum and the diffraction reflection angle, respectively. The silver crystallite size was D = 21.5(1) nm.

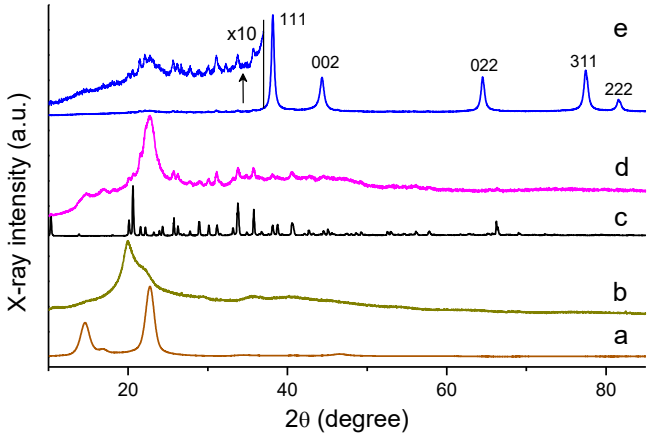


Figure 2 Diffraction patterns of BC (a), Chit (b), GA (c), BC-Chit-GA (d) and BC-Chit-GA@Ag (e). (e) shows the Miller indices of the reflections of the metallic Ag phase.

Surface composition control is an important factor for medical materials. XPS not only assesses the purity of composites but also characterizes the various chemical states of atoms in the near-surface region of materials (5-10 nm).

Survey spectra of BC-Chit-GA@Ag demonstrated the absence of impurities in the composite. Figure 3 shows the N 1s photoelectron spectra of Chit and BC-Chit-GA@Ag composite, and Table S1 lists their characteristics.

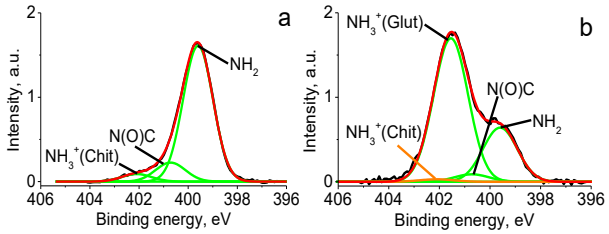


Figure 3 XPS N 1s spectra of samples: Chit(a) and BC-Chit-GA@Ag(b)

In the N 1s spectrum of Chit, the peak at a binding energy of 399.6 eV is characteristic of chitosan, whereas the peak at 400.7 eV corresponds to chitin. [27] For BC-Chit-GA@Ag, an additional peak at a binding energy of 401.5 eV was observed, which can be attributed to the NH3+ group of glutamic acid. [28] Analysis of the C 1s spectra of the Ch and Ch@Ag-GA samples revealed significant differences in the intensity of the peak at 288.7 eV, corresponding to the C(O)N group. The content of the C(O)N group in the Ch@Ag-GA sample increased fourfold following the interaction between chitosan and glutamic acid; this can be attributed to the cross-linking of chitosan with glutamic acid (Fig. S5 and Table S2).

In the BC-Chit-GA@Ag spectrum, the peak width was 1.6 eV, whereas for Chit it was 1.4 eV. The slight increase in width may be attributed to the heterogeneity of the Ag-containing composite, resulting in a less uniform charge distribution on the surface. Figure 4 shows the Ag 3d photoelectron spectrum

© Mendeleev Communications.

of the BC-Chit-GA@Ag composite, and Table S3 presents its characteristics.

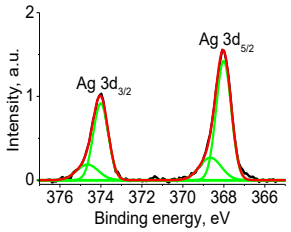


Figure 4 Photoelectron spectra of Ag 3d sample BC-Chit-GA@Ag

The Ag 3d spectrum of the BC-Chit-GA@Ag composite (Figure 4) was approximated by two spin-orbit doublets Ag $3d_{5/2}$–Ag $3d_{3/2}$ centered at 368.0–374.0 and 368.7–374.7 eV (Table S2). According to the literature, the average binding energies of silver for Ag^0, Ag_2O, and AgO in the Ag $3d_{5/2}$ peak are 368.2, 367.8, and 367.4 eV.[29] The first peak of Ag $3d_{5/2}$ at 368.0 eV is located between Ag_2O (367.8 eV) and Ag^0 (368.2 eV) and the electron energy of Ag $3d_{5/2}$ of the second peak (368.7 eV) is higher than that of unoxidized silver. Analysis of the results obtained allows us to assign a binding energy of 368.0 eV to the Ag^+ state, and 368.7 eV to Ag^0.

Hybrid Ag-containing materials based on bacterial cellulose, chitosan and glutamic acid were obtained using metal-steam synthesis, gelation and lyophilization methods. Metal nanoparticles in the composite are in the Ag^0 and Ag^+ states. The porous metal polymer has a three-dimensional network structure, the framework of which is formed by bacterial cellulose, and glutamic acid is a cross-linking agent of chitosan. The material may be promising for medical applications as wound dressings.

This work was supported by State Assignment № 075-03-2026-024 of the Ministry of Science and Higher Education of the Russian Federation. The authors thank the Center for Molecular Structure Research in the Institute of Organoelectronics and Electronics of the Russian Academy of Sciences and K. Borisov for the SEM studies.

Online Supplementary Materials

Supplementary data associated with this article can be found in the online version at doi: 10.71267/mencom.8216

References

1 R. Urban-Chmiel, A. Marek, D. Stępień-Pyśniak, K. Wieczorek, M. Dec, A. Nowaczek and J. Osek, *Antibiotics*, 2022, **11**, 1079; https://doi.org/10.3390/antibiotics11081079.

2 R. Aggarwal, P. Mahajan, S. Pandiya, A. Bajaj, S. K. Verma, P. Yadav, A. S. Kharat, A. U. Khan, M. Dua, and A.K. Johri, *Crit. Rev. Microbiol.*, 2024, **50**, 896; https://doi.org/10.1080/1040841X.2024.2313024.

3 O. Asanarong, V. Minh Quan, S. Boonrungsiman and P. Sukyai, *Eur. Polym. J.*, 2021, **143**, 110224; https://doi.org/10.1016/j.eurpolymj.2020.110224.

4 L. Deng, B. Wang, W. Li, Z. Han, S. Chen and H. Wang, *Int. J. Biol. Macromol.*, 2022, **217**, 77; https://doi.org/10.1016/j.ijbiomac.2022.07.017.

5 A. Zeng, R. Yang, Y. Tong and W. Zhao, *Int. J. Biol. Macromol.* 2023, **235**, 123739; https://doi.org/10.1016/j.ijbiomac.2023.123739.

6 S. Zhou, H. Peng, A. Zhao, R. Zhang, T. Li, X. Yang and D. Lin, *Int. J. Biol. Macromol.*, 2024, **259**, 129392. https://doi.org/10.1016/j.ijbiomac.2024.129392.

7 M. G. Chernysheva, T. Shen, I. S. Chaschin, G. A. Badun, V. G. Vasil'ev, I. V. Mikheev and N. P. Bakuleva, *Mendeleev Commun.*, 2024, **34**, 104; https://doi.org/10.1016/j.mencom.2024.01.031106.

8 M. Rubina, A. Vasil'kov and V. Sadykova. *Patent RF 2 804 241 C1*, 2023; https://fips.ru/EGD/000faed4-49ac-49a8-8973-13c2886a2daf

9 H. Zhao, L. Zhang, S. Zheng, S. Chai, J. Wei, L. Zhong, Y. He and J. Xue, J. *Carbohydr. Polym.*, 2022, **281**, 119017; https://doi.org/10.1016/j.carbpol.2021.119017.

10 Y. Anwar, M. Ul-Islam, H. S. H. Mohammed Ali, I. Ullah, A. Khalil and T. Kamal, *J. Mater. Res. Technol.*, 2022, **18**, 2037; https://doi.org/10.1016/j.jmrt.2022.03.089.

11 X. Liu, Z. Cai, M. Pei, H. Zeng, L. Yang, W. Cao, X. Zhou and F. Chen, *Adv. Healthc. Mater.*, 2024, **13**, e2302893; https://doi.org/10.1002/adhm.202302893.

12 X. Che, T. Zhao, J. Hu, K. Yang, N. Ma, A. Li, Q. Sun, C. Ding and Q. Ding, *Polym.*, 2024, **16**, 344; https://doi.org/10.3390/polym16030344.

13 D. Lahiri, M. Nag, B. Dutta, A. Dey, T. Sarkar, S. Pati, H. A. Edinur, Z. Abdul Kari, N. H. Mohd Noor and R. R. Ray, *Int. J. Mol. Sci.*, 2021, **22**, 12984; https://doi.org/10.3390/ijms222312984.

14 L. Wang, L. Du, M. Wang, X. Wang, S. Tian, Y. Chen, X. Wang, J. Zhang, J. Nie and G. Ma, *Carbohydr. Polym.*, 2022, ***285***, 119209; https://doi.org/10.1016/j.carbpol.2022.119209.

15 K. Liu, Y. Wang, W. Liu, C. Zheng, T. Xu, H. Du, Z. Yuan and C. Si, *Chem. Eng. J.*, 2024, **494**, 153014; https://doi.org/10.1016/j.cej.2024.153014.

16 L. Urbina, O. Guaresti, J. Requies, N. Gabilondo, A. Eceiza, M. A. Corcuera and A. Retegi, *Carbohydr. Polym.*, 2018, **193**, 362; https://doi.org/10.1016/j.carbpol.2018.04.007.

17 P. Thangavel, B. Ramachandran, S. Chakraborty, R. Kannan, S. Lonchin and V. Muthuvijayan, *Sci. Rep.*, 2017, **7**, 10701; https://doi.org/10.1038/s41598-017-10882-1.

18 C. Meng, J. Hu, K. Gourlay, C. Yu and J. N. Saddler, *Cellulose*, 2019, **26**, 8325; https://doi.org/10.1007/s10570-019-02446-5.

19 R. I. Dovnar, A. Y. Vasil'kov, S. M. Smotryn, N. N. Iaskevich, *Patent BY 12964 U*, 2022; https://ncip.by/upload/iblock/e4f/e4fe41f2b826eb4abcb7fd6613fb0552.pdf

20 A. A. Voronova, A. V. Naumkin, A. Yu. Pereyaslavtsev, T. Batsalova, B. Dzhambazov and A. Yu. Vasil'kov, *Dokl. Phys. Chem.*, 2024, **514**, 1; https://doi.org/10.1134/S0012501624600025.

21 A. Yu. Vasil'kov, P. R. Voloshina, A. V. Naumkin and N. S. Molcheva. Russ. Chem. Bull., 2026, **75**, 1—8. https://doi.org/...

22 A. N. Tretyakova, P. R. Voloshina, A. V. Naumkin, A. Y. Pereyaslavtsev, N. A. Arkharova, V. V. Volkov, E. V. Shtykova and A. Y. Vasil'kov, *Mendeleev Commun.*, 2025, **35**, 481; https://doi.org/10.71267/mencom.7706.

23 V. V. Zefirov, V. S. Sadykova, I. P. Ivanenko, O. P. Kuznetsova, I. E. Butenko, T. I. Gromovykh and O. I. Kiselyova, *Carbohydr. Polym.*, 2022, **292**, 119692; https://doi.org/10.1016/j.carbpol.2022.119692.

24 A. Vasil'kov, I. Butenko, A. Naumkin, A. Voronova, A. Golub, M. Buzin, E. Shtykova, V. Volkov and V. Sadykova, *Int. J. Mol. Sci.*, 2023, **24**, 7667; https://doi.org/10.3390/ijms24087667.

25 T. Wang, H. Yang, J. D. Kubicki and M. Hong, *Biomacromolecules*, 2016, **17**, 2210; https://doi.org/10.1021/acs.biomac.6b00441.

26 G. Hao, Y. Hu, L. Shi, J. Chen, A. Cui, W. Weng and K. Osako, *Sci Rep*, 2021, **11**, 1646; https://doi.org/10.1038/s41598-021-81318-0.

27 I. V. Novikov, M. A. Pigaleva, E. E. Levin, S. S. Abramchuk, A. V. Naumkin, H. Li, A. Pich and M. O. Gallyamov, *Colloid Polym. Sci*,. 2020, **298**, 1135; https://doi.org/10.1007/s00396-020-04683-8.

28 J. S. Stevens, A. C. de Luca, M. Pelendritis, G. Terenghi, S. Downes and S. L. M. Schroeder, *Surf. Interface Anal.*, 2013, **45**, 1238; https://doi.org/10.1002/sia.5261.

29 G. B. Hoflund, J. F. Weaver and W. S. Epling, *Surf. Sci. Spectra*, 1994, **3**, 163; https://doi.org/10.1116/1.1247779.

Received: 30th September 2026; Com. 26/8216

© Mendeleev Communications.